Contribution from the Department of Chemistry and Biochemistry, University of California at Los Angeles, Los Angeles, California 90024

Photochemistry and Single-Crystal Polarized Absorption Spectroscopy of (η^4-Cyclooctatetraene)tricarbonyliron

TSU-HSIN CHANG and JEFFREY I. ZINK*

Received October 26, 1984

The wavelength-dependent photosubstitution reactions of (η^4-cyclooctatetraene)tricarbonyliron in cyclohexane are studied. All of the quantum yields increase with decreasing wavelengths of the irradiation between 488 and 366 nm but then decrease at 334 nm. The electronic excited states responsible for the photoreactivity are assigned by using single-crystal polarized electronic absorption spectroscopy. The trends in the wavelength-dependent photoreactivity correlate with the trends in excited-state antibonding changes, which are determined from angular overlap theory.

Introduction

The photochemistry of (diene)tricarbonyliron compounds has been the subject of several recent studies, both in solution phase[1] and in matrices.[2,3] The general conclusion which can be drawn from these studies is that both carbonyl and olefin labilization take place with wavelength-dependent quantum yields. In the solution-phase studies, the ligand substitution quantum yields for a variety of substituted dientricarbonyliron compounds (not including η^4-cyclooctatetraene, COT) were measured.[1] The quantum yield for both CO and diene loss increased with increasing irradiation energy. The comparatively low observed quantum yields for diene loss were attributed to formation of η^2-diene intermediates, which predominantly re-form the starting material. In the matrix studies, η^2-coordination was directly detected by IR spectroscopy. In the work most relevant to this paper, Rest, et al. observed (η^4-COT)$Fe(CO)_2$, (η^2-COT)$Fe(CO)_3$, and the "chair" conformation of (η^4-COT)$Fe(CO)_3$ in methane matrices.[4]

The excited electronic states giving rise to the photochemical reactions have not been studied. The electronic absorption spectrum in solution is known to contain low-intensity features at wavelengths longer than about 310 nm and intense features at shorter wavelengths.[5] No further details are known.

In this paper we report the wavelength-dependent CO and olefin photosubstitution quantum yields of Fe(η^4-COT)$(CO)_3$. The electronic spectrum, including polarization studies, is reported, and the lowest energy excited states are assigned. The wavelength dependence of the ligand exchange quantum yields is explained in terms of the state assignments.

Experimental Section

Photochemistry. The light source for the photochemical studies at 334, 366, 406, and 436 nm was a 1000-W Hanovia high-pressure mercury lamp. The individual mercury lines were isolated by using appropriate solution and glass filters. An argon ion laser was used for the 488-nm excitation. Light intensities were measured with ferrioxalate actinometry.[6]

All photochemical reactions were run in cyclohexane under a nitrogen atmosphere. The concentration of $Fe(COT)(CO)_3$ was 2.0×10^{-3} M in all quantum yield measurements. The concentration of the entering ligand, $P(OMe)_3$, was 2.0×10^{-2} M in all cases. Reactions were carried out to less than 15% completion in round, stirred, 1-cm path length quartz cells mounted in a thermostated block. The spectra and the absorbance vs. concentration working curves obeyed Beer's law within the concentration range that was studied (0 to 2.0×10^{-3} M). No measured thermal reaction occurred within 24 h.

Spectroscopy. All IR spectra were recorded by using a Perkin-Elmer 621 IR spectrometer. The room-temperature and 77 K glass absorption spectra were recorded on a Cary 14 spectrometer. The methylcyclohexane glass spectra were obtained by using an optical Dewar filled with liquid nitrogen. The 12 K single-crystal polarized absorption spectra were obtained on a locally constructed instrument, which has been described previously.[7] Single crystals exhibiting beautiful linear pleochroism and having dimensions of approximately 20×50 μm were grown by slow evaporation of a cyclohexane solution from between two quartz plates.

Materials. (η^4-COT)$Fe(CO)_3$ was prepared according to the published method.[5] The cyclohexane solvent was dried over $CaCl_2$ and freshly distilled under nitrogen before use.[8] $P(OMe)_3$ was freshly distilled under nitrogen before use.[8] A sample of (η^4-COT)$Fe(CO)_2(P(OMe)_3)$ was prepared by irradiating a mixture of (COT)$Fe(CO)_3$ and $P(OMe)_3$ in cyclohexane for 48 h with a 600-W Hg/Xe lamp. The reaction mixture was concentrated and eluted with a 2:1 ratio of cyclohexane and benzene through a column of silica gel. The product was obtained as a yellow liquid.

Results

The photosubstitution products of the reaction of (η^4-COT)$Fe(CO)_3$ with the Lewis base ligand $P(OMe)_3$ were identified by their characteristic IR bands. The carbonyl stretching region proved to be the most informative. In the initial runs to identify the products, 0.01 M (COT)$Fe(CO)_3$ and 0.1 M $P(OMe)_3$ in cyclohexane were irradiated in a 0.5-mm NaCl IR cell with 366-nm light.

When irradiation began, only the bands at 2053, 1992, and 1975 cm^{-1} were observed. As the irradiation progressed, these three bands from the starting material steadily decreased in intensity. The first new bands appeared at 1946 and 1939 cm^{-1} followed by the appearance of bands at 1919 and 1910 cm^{-1}. After prolonged irradiation, a band appeared at 1875 cm^{-1} and steadily increased in intensity while the 1946, 1939, 1919, and 1910 cm^{-1} bands decreased.

The photoproducts were identified by comparing the new bands with those from independently prepared samples and/or those reported in the literature.[9,10] The two peaks at 1946 and 1939 cm^{-1} are from (COT)$Fe(CO)_2P(OMe)_3$. These peaks are almost identical with those reported for (butadiene)$Fe(CO)_2P(OMe)_3$ at 1943 and 1936 cm^{-1} and those found in an independently prepared sample. The two peaks at 1919 and 1910 cm^{-1} are from $Fe(CO)_3(P(OMe)_3)_2$.[9] The peak at 1875 cm^{-1} is from $Fe(CO)_2(P(OMe)_3)_3$.[10] The higher energy peaks from these compounds are obscured by the intense 2053- and 1992-cm^{-1} peaks of the starting material.

The first photoproduct observed is (COT)$Fe(CO)_2P(OMe)_3$, which is formed by carbonyl loss. The next photoproduct, $Fe(CO)_3(P(OMe)_3)_2$, is formed after loss of the cyclooctatetraene.

(1) Jaenicke, C.; Kerber, K. C.; Kirsch, P.; Koerner von Gustorf, E. A.; Rumin, R. *J. Organomet. Chem.* **1980**, *187*, 361.
(2) Ellerhorst, G.; Gerhartz, W.; Grevels, F.-W. *Inorg. Chem.* **1980**, *19*, 67.
(3) Goggin, P. L.; Goodfellow, R. J.; et al. *J. Chem. Soc., Dalton Trans.* **1977**, 2061.
(4) Rest, A. J., private communication on the photochemistry of (COT)$Fe(CO)_3$ in the methane matrix.
(5) Manuel, T. A.; Stone, F. G. A. *J. Am. Chem. Soc.* **1960**, *82*, 366.
(6) Calvert, J. G.; Pitts, J. N., Jr. "Photochemistry"; Wiley: New York, 1966.
(7) Change, T.-H.; Zink, J. I. *J. Am. Chem. Soc.* **1984**, *106*, 287.
(8) Jolly, W. L. "The Synthesis and Characterization of Inorganic Compounds"; Prentice-Hall: Englewood Cliffs, NJ, 1970; Chapter 2.
(9) VanDerveer, M. C.; Burlitch, J. M. *J. Organomet. Chem.* **1980**, *197*, 357.
(10) Harris, T. V.; Rathke, J. W.; Muetterties, E. L. *J. Am. Chem. Soc.* **1978**, *100*, 6966.

0020-1669/85/1324-4016$01.50/0

Table I. Photochemical Quantum Yields

	λ,[a] nm				
	334	366	406	436	488
Φ_{dis}[b]	0.034	0.101	0.023	0.013	0.008
Φ_{CO}[c]	0.018	0.076	0.016	0.010	0.004
Φ_{COT}[d]	0.016	0.025	0.007	0.003	0.004

[a] Excitation wavelength. [b] Disappearance quantum yields for the starting material. [c] Quantum yields for CO substitution by P(OMe)$_3$. [d] Quantum yields for COT substitution, obtained from the difference between Φ_{dis} and Φ_{CO}.

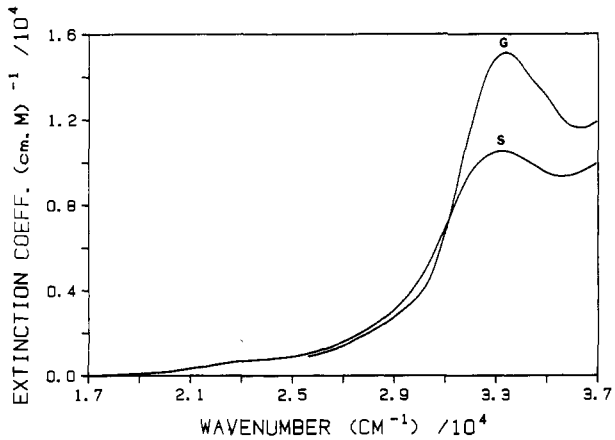

Figure 1. Absorption spectrum of (COT)Fe(CO)$_3$ in methylcyclohexane at room temperature in solution (s) and at liquid-nitrogen temperature in a glass (G).

A secondary photoproduct, Fe(CO)$_2$(P(OMe)$_3$)$_3$, is formed after loss of a carbonyl from Fe(CO)$_3$(P(OMe)$_3$)$_2$ and/or loss of the COT from (COT)Fe(CO)$_2$P(OMe)$_3$. These reactions are summarized as follows:

Primary Photoproducts

$$(COT)Fe(CO)_3 + P(OMe)_3 \xrightarrow{h\nu} (COT)Fe(CO)_2P(OMe)_3 + CO$$

$$(COT)Fe(CO)_3 + 2P(OMe)_3 \xrightarrow{h\nu} \textit{trans}\text{-}Fe(CO)_3(P(OMe)_3)_2 + COT$$

Secondary Photoproducts

$$(COT)Fe(CO)_2P(OMe)_3 + 2P(OMe)_3 \xrightarrow{h\nu} Fe(CO)_2(P(OMe)_3)_3 + COT$$

$$Fe(CO)_3(P(OMe)_3)_2 + P(OMe)_3 \xrightarrow{h\nu} Fe(CO)_2(P(OMe)_3)_3 + CO$$

The quantum yields for the formation of the primary photoproducts and for the disappearance of the starting material were studied as a function of wavelength. Concentrations were determined from a working curve of IR absorbance vs. concentration. All bands obeyed Beer's law up to the highest concentration studied, 0.002 M. All plots passed through the origin with the following slopes S: 1992 cm^{-1}, S = 380; 1975 cm^{-1}, S = 283; 2053 cm^{-1}, S = 250; 1939 cm^{-1}, S = 144; 1997 cm^{-1}, S = 107; 1946 cm^{-1}, S = 63. The quantum yields as a function of excitation wavelengths are given in Table I.

The quantum yields all increase with decreasing wavelength of irradiation from 488 to 366 nm and then decrease at 334 nm. The ratio of CO loss to COT loss increases from 1 to 3 from 488 to 366 nm and then decreases to 1. The total reactivity is more than a factor of 3 higher at 366 nm than that at any of the other excitation wavelengths.

Electronic Absorption Spectra

The room-temperature electronic absorption spectra of (COT)Fe(CO)$_3$ in methylcyclohexane is shown in Figure 1. The dominant feature is the peak at 33 000 cm^{-1}. The long featureless tail on the low-energy side consists of unresolved d–d bands (vide infra) out to about 23 000 cm^{-1}.

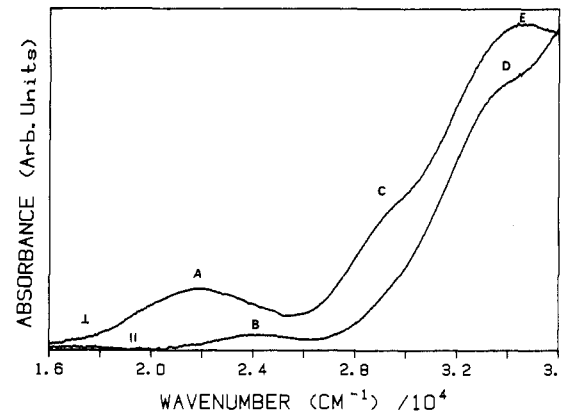

Figure 2. Polarized electronic absorption spectra of a single crystal of (COT)Fe(CO)$_3$ at 10 K. The spectra are from a type 1 crystal with the electric vector of the incident light parallel and perpendicular to the a direction.

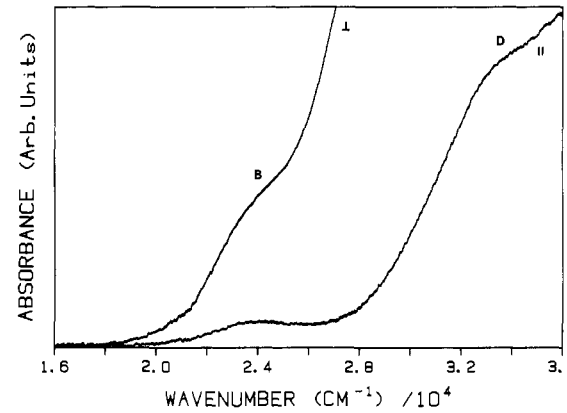

Figure 3. Polarized electronic absorption spectra of a single crystal of (COT)Fe(CO)$_3$ at 10 K. The spectra are from a type 2 crystal with the electric vector of the incident radiation parallel and perpendicular to the a direction.

The liquid-nitrogen-temperature spectrum in a methylcyclohexane glass is also shown in Figure 1. The 33 000-cm^{-1} peak becomes sharper, and some poorly resolved features are observed on it at 35 000 cm^{-1}. The long tail to lower energy remains unresolved although the shoulder at about 30 000 cm^{-1} becomes more apparent.

The individual low-energy features were resolved and identified by using single-crystal polarized absorption spectroscopy at 10 K. In order to obtain the crystal spectra, microcrystals having thicknesses on the order of 10^3 Å had to be used. Two different types of single crystals presenting different crystal faces were obtained when the crystals were grown from cyclohexane and from dichloromethane solutions. These crystals will be called type 1 and type 2, respectively.

Single crystals of type 1 formed long narrow plates. When viewed under polarized light with a polarizing microscope, they appeared green when the polarization direction was along the extinction direction at an angle of 3.5° to the long crystal axis. They appeared red in the orthogonal direction. The crystals presented the *ac* face with the long axis corresponding to the *a* direction (vide infra). The 10 K absorption spectra are shown in Figure 2. The parallel spectrum was obtained with the electric vector of the incident light at a 3.5 angle to the long crystal axis. The perpendicular spectrum was obtained in the orthogonal direction. Five features are observed from this face in the region between 16 000 and 36 000 cm^{-1}. Two completely resolved bands, bands A and B, are observed at 21 800 and 24 000 cm^{-1} with opposite polarizations. The next higher energy bands are the shoulder C at about 28 900 cm^{-1} and the shoulder D at 33 200

Table II

Experimental Transition Energies and Polarizations and Excited-State Assignments

abs max, cm^{-1}	polarizn	assignt	label[a]
21 800	z	$(^1A'')\ d_{z^2} \rightarrow d_{xy}$	A
24 000	x,y	$(^1A')\ d_{xz} \rightarrow d_{xy}$	B
28 900	z	$(^1A'')\ d_{yz} \rightarrow d_{xy}$	C
33 200	x,y	$(^1A')\ d_{z^2} \rightarrow \pi^*$(olefin)	D
34 400	z	$(^1A'')\ d_{x^2-y^2} \rightarrow d_{xy}$	E

Electric Dipole Selection Rules in the C_s Point Group

transition	c (z)	a (x)	b (y)
$^1A' \rightarrow {}^1A'$	forbidden	allowed	allowed
$^1A' \rightarrow {}^1A''$	allowed	forbidden	forbidden

[a] From Figures 2 and 3.

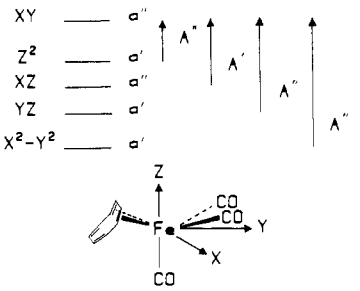

Figure 4. Axis system, orbitals, and states important in the spectroscopy and photochemistry of $(COT)Fe(CO)_3$. The irreducible representations of the d orbitals (lower case letters) and of the excited states corresponding to the one-electron transitions (capital letters) are shown.

cm^{-1}. Shoulder C has the same polarization as the lowest energy band. The intense band at 34 400 cm^{-1} corresponds to the shoulder at 35 000 cm^{-1} in the glass spectrum.

Single crystals of type 2 have a characteristic angle of 25.5° between the long crystal edge and the adjacent edge. This type of crystal presented the *ab* face. The 10 K absorption spectra are shown in Figure 3. The parallel spectrum was obtained with the electric vector of the incident radiation parallel to the extinction direction at an angle of 1.3° to the long crystal axis, which is the crystallographic *a* axis. The perpendicular spectrum was obtained in the orthogonal extinction direction perpendicular to the x axis. The parallel spectrum is the same as that observed in the parallel spectrum in Figure 2 from the type 1 crystals. Only one band, the shoulder B at 24 000 cm^{-1}, was observed in the perpendicular spectrum. The selection rules and the assignments of these bands will be discussed in the next section. The data are summarized in Table II.

Discussion

1. Excited-State Assignments. The molecular geometry and the coordinate system to be used in the following discussion are shown in Figure 4. The $(COT)Fe(CO)_3$ molecule has C_s symmetry with the mirror plane in the yz plane. In the solid state, it crystallizes the *Pnam* space group with the mirror plane containing the *a* and *b* crystal axes.[11]

The irreducible representations of the individual d orbitals and the excited-state symmetries are shown in Figure 4. The ground electronic state, corresponding to a $(d_{x^2-y^2})^2(d_{yz})^2(d_{xz})^2(d_{z^2})^2$ electron configuration, transforms a $^1A'$. The irreducible representations of the excited states corresponding to the one-electron transitions to the empty d_{xy} orbital are shown next to the arrows representing the transitions in Figure 4. The x component of the electric dipole operator transforms as A'' and the y and z components as A'. Thus the A' to A' transition is y and z allowed and the A' to A'' transition is x allowed.

The contribution of the individual ligands to the orbital and the state energies can be difficult to interpret in complexes of low symmetry. A simple interpretation is provided by the angular overlap model.[12,13] The crystallographically determined positions of the ligands are used.[11] The σ and π contributions from the COT ligand are calculated along the lines of the Dewar–Chatt model.[14,15] The midpoint of the C=C unit is assumed to be the coordinate for the origin of the "σ" contribution from the filled ligand pi orbital and the "π-acceptor" contribution from the empty π-antibonding orbital. All three of the AOM coordinates including the ψ "twist" angle are obtained from the crystallographically determined atomic positions. The calculated d orbital energies and the diagonal expressions for the transition energies are shown in Table III.

Table III. Contributions of the Bonding Interactions to the d-Orbital Energies (Top) and Transition Energies (Bottom)

	e_σ^{CO}	e_π^{CO}	e_σ^{CC}	e_π^{CC}
d_{xy}	1.39	0.08	0.79	0.00
d_{z^2}	1.40	0.20	0.00	0.49
d_{xz}	0.11	1.97	0.21	0.00
d_{yz}	0.09	1.83	0.00	0.34
$d_{x^2-y^2}$	0.01	1.92	0.00	0.16

$(d_{z^2} \rightarrow d_{xy})\ \Delta E_1 = -4B - C - 0.014e_\sigma^{CO} - 0.12e_\pi^{CO} + 0.79e_\sigma^{CC} - 0.49e_\pi^{CC}$

$(d_{xz} \rightarrow d_{xy})\ \Delta E_2 = -3B - C + 1.28e_\sigma^{CO} - 1.89e_\pi^{CO} + 0.59e_\sigma^{CC}$

$(d_{yz} \rightarrow d_{xy})\ \Delta E_3 = -3B - C + 1.30e_\sigma^{CO} - 1.75e_\pi^{CO} + 0.79e_\sigma^{CC} - 0.34e_\pi^{CC}$

$(d_{x^2-y^2} \rightarrow d_{xy})\ \Delta E_4 = -C + 1.38e_\sigma^{CO} - 1.84e_\pi^{CO} + 0.79e_\sigma^{CC} - 0.16e_\pi^{CC}$

[a] The e_σ and e_π values are the AOM σ and π parameters. The superscripts CO and CC refer to the carbonyl ligand and a C=C part of the COT ligand, respectively. The e_σ values are positive. For π-acceptor ligands, $e_\pi < 0$.

The assignments of the lowest energy ligand field transitions shown in Figure 4 can be made on the basis of the polarization properties. In the spectrum shown in Figure 2, three bands, bands A through C, are polarized perpendicular to the long axis of the crystal while the middle peak, band B, is polarized parallel to the long axis of the crystal. On the basis of the group theoretical selection rules, the xz to xy, $^1A'$ to $^1A'$, transition is polarized opposite to all of the other transitions. Thus, the polarization of band B, which is opposite to that of the other bands, identifies band B as the transition to the $^1A'$ excited state. The lowest energy absorption band is then immediately assigned to the $^1A'$ to $^1A''$, z^2 to xy, transition. The energy of this transition is almost independent of the σ and π interactions with the carbonyl ligands (Table III). The assignment of bands C and E cannot be unambiguously made because the two remaining transitions are expected to have roughly similar energies and have the same polarizations. Both of these transitions have roughly equal σ and π coefficients from the carbonyl ligands and differ primarily in the contribution of the olefin π back-bonding and the Racah parameters to the energy. On the basis of the lower electron repulsion energy and slightly lower carbonyl σ coefficient, band C is tentatively assigned to the $d_{x^2-y^2} \rightarrow d_{xy}$ transition.

The most intense feature in the electronic absorption spectrum is the band at 33 200 cm^{-1}. On the basis of its intensity ($\epsilon > 10^4$ in solution), it is assigned to a charge-transfer transition. It is allowed in perpendicular polarization in Figure 2, i.e. in the y direction, and thus is assigned to a $^1A' \rightarrow {}^1A'$ transition. Its relatively lower intensity in parallel (x) polarization probably is a result of the small transition dipole moment in that direction. Two possibilities for the charge transfer are plausible: iron to carbonyl or iron to olefin charge transfer. Two independent pieces of evidence suggest that the latter assignment is correct. First, an INDO calculation shows that the three COT π orbitals lie

(11) Dickens, B.; Lipscomb, W. N. *J. Chem. Phys.* **1962**, *37*, 2084.
(12) Jørgensen, C. K.; Pappalardo, R.; Schmidtke, H. H. *J. Chem. Phys.* **1963**, *39*, 1422. Schaffer, C. E.; Jørgensen, C. K. *Mol. Phys.* **1965**, *9*, 401.
(13) Gerloch, M.; Slade, R. C. "Ligand Field Parameters"; Cambridge University Press: London, 1973.
(14) Dewar, M. J. S. *Bull. Soc. Chim. Fr.* **1951**, *18*, C71.
(15) Chatt, J.; Duncanson, L. A. *J. Chem. Soc.* **1953**, 2939.

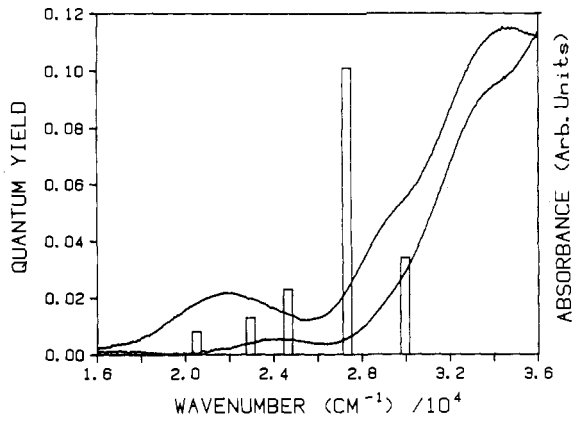

Figure 5. Superposition of the photochemical quantum yields, shown by the vertical bars, on the electronic absorption spectrum.

directly above the iron 3d orbitals.[16] Thus, according to the INDO calculation, the iron to COT charge-transfer band should be lower in energy than the iron to CO band. Second, experimental studies of the parent compound, $Fe(CO)_5$, show that the lowest energy metal to CO charge-transfer band occurs at 41 500 cm^{-1}, much higher in energy than the observed 33 200-cm^{-1} band.[17] For these reasons, we tentatively assign the 33 200-cm^{-1} band to an iron to olefin charge transfer.

2. Wavelength-Dependent Photoreactivity. The photochemical reactivity of (COT)Fe(CO)$_3$ is similar in many respects to that of other olefin complexes of iron carbonyl. The quantum yield for ligand substitution is highly wavelength-dependent, and both olefin and carbonyl substitution are observed. However, the reactivity reported here differs from that of other olefin complexes of iron in that the quantum yield increases, reaches a maximum, and then decreases with decreasing wavelength of irradiation. The quantum yields and wavelength dependences are given in Table I. The relationship between the quantum yields and the absorption spectrum is shown in Figure 5.

The trends in the wavelength dependence of the photochemical quantum yields are correlated with the trends in the bonding changes between the ground and excited electronic states. The electronic absorption spectra and the spectral assignments discussed previously help to present a bonding explanation of the reactivity patterns.

The lowest excited electronic state in Figure 4 is $^1A''$, d_{z^2} to d_{xy}. This transition corresponds to a transition from an orbital that is primarily σ antibonding between the metal and the ligands to another that is primarily σ antibonding (cf. the coordinate system in Figure 4). Thus, as shown in Table III, there is almost no change in the σ bonding between the metal and a CO ligand when this excited state is populated. The coefficient representing this change is only −0.01. The changes in the π bonding are likewise relatively small (−0.12 for the π-bonding change between the metal and the carbonyl ligand and −0.49 for that between the metal and olefin). The largest of the changes is the metal–olefin σ bonding (0.79). None of these changes is very large. Thus the quantum yield is relatively small when this state is populated by using 488-nm irradiation.

The second lowest excited electronic state in Figure 4 is $^1A'$, d_{xz} to d_{xy}. The bonding changes that occur when this state is populated are larger than those of the previous state. The major bonding changes weaken the metal–carbonyl σ and π bonds (coefficients 1.28 and −1.89, respectively). However, the absorption band corresponding to this transition is overlapped on both sides by other d–d transitions and has a lower extinction coefficient than these other transitions. Thus, it is impossible to directly and selectively populate only this state. Irradiation at 436 and 406 nm can populate this state, but most of the light is absorbed by the more intense band at lower energy. From Figure 5, the most efficient wavelength for maximizing the absorbance into this state is about 406 nm. The quantum yield for CO substitution increases dramatically at both 406 and 436 nm relative to that at 488 nm. The quantum yield for COT loss remains small. These observations are in accord with the increased metal–carbonyl bond weakening in the $^1A'$ excited state.

The next higher energy excited state is $^1A''$, but its orbital components cannot be unambiguously assigned. It is either d_{yz} or $d_{x^2-y^2}$ to d_{xy}. In both of these cases, large bonding weakenings between the metal and carbonyl ligands occur and increased carbonyl substitution is expected. The increase in the olefin substitution quantum yield is surprising because the expected bond weakenings are about the same as those discussed previously. As was the case for the previous state, this state is overlapped on both sides, to low energy by the $^1A'$ state and to high energy by the charge-transfer state. The overlap by the lowest energy transition becomes minor. Thus, at 366-nm irradiation both carbonyl substitution and olefin substitution are observed with the larger quantum yields for disappearance of the starting material attributed to the negligible overlap by the photoinert excited state.

At the shortest wavelengths studied, the spectrum is dominated by the intense tail of the charge-transfer transition. The bond weakenings caused by populating this state cannot be inferred from the angular overlap model coefficients. The experimentally observed decrease in the ligand substitution quantum yields suggests that bonding changes in this charge-transfer state do not dominate the photochemistry, either because the changes are small or because some other excited-state deactivation mechanism becomes important. The decreased observed reactivity, when contrasted with the increased reactivity reported for other diolefins, suggests the possibility that the larger and cyclic olefin ligand offers increased deactivation pathways.

Acknowledgment. The support of this research by the National Science Foundation is gratefully acknowledged.

Registry No. COT, 629-20-9; (COT)Fe(CO)$_2$P(OMe)$_3$, 73130-77-5; *trans*-Fe(CO)$_3$(P(OMe)$_3$)$_2$, 19457-84-2; Fe(CO)$_2$(P(OMe)$_3$)$_3$, 14767-99-8; (COT)Fe(CO)$_3$, 78147-28-1; CO, 630-08-0; P(OMe)$_3$, 121-45-9.

(16) Bohm, M. C.; Gleiter, R. *Z. Naturforsch., B: Anorg. Chem., Org. Chem.* **1980**, *35B*, 1028.
(17) Dartiguenave, M.; Dartiguenave, Y.; Gray, H. B. *Bull. Soc. Chim. Fr.* **1969**, *12*, 4223.